

Linking atmospheric dimethyl sulfide and the Arctic Ocean spring bloom

Ki-Tae Park,¹ Kitack Lee,¹ Young-Jun Yoon,² Hyun-Woo Lee,¹ Hyun-Cheol Kim,² Bang-Yong Lee,² Ove Hermansen,³ Tae-Wook Kim,¹ and Kim Holmén⁴

Received 9 November 2012; revised 21 November 2012; accepted 29 November 2012; published 16 January 2013.

[1] We measured atmospheric dimethyl sulfide (DMS) mixing ratios at approximately hourly intervals over a 1 year period (April 2010 to March 2011) in the Atlantic sector of the Arctic Ocean (Svalbard, Norway; 78.5°N, 11.8°E). The mixing ratios varied by several orders of magnitude over time scales of less than several days, and occasionally reached 200–300 parts per trillion by volume during the major phytoplankton growth period (May to September), whereas during the winter months (October to April) the mixing ratios were on the order of a few parts per trillion by volume. Our results, based on analyses using multiple data products (atmospheric DMS mixing ratios, satellite-derived ocean colors, and meteorological datasets), indicated that weekly variability in the DMS mixing ratios at Svalbard was highly correlated with variability in the chl-*a* concentration in waters in the vicinity of Svalbard ($r=0.89$). Hourly-to-daily variability in the DMS mixing ratios were satisfactorily explained by changes in the trajectory, altitude, and speed of air masses passing the DMS sources prior to reaching Svalbard. The observed coupling between DMS mixing ratios and chl-*a* concentration is surprising, and indicates that the variability in chl-*a* concentrations in the study area represents the change in the abundance of phytoplankton capable of producing DMS. The intensive monitoring of DMS levels at Svalbard enabled us to identify in situ production and the flux of oceanic DMS over the Arctic region. It thus constitutes a useful analytical tool for detecting changes in DMS production associated with variations in phytoplankton productivity resulting from changes in sea ice extent as a consequence of Arctic seasonality and warming. **Citation:** Park, K.-T., K. Lee, Y.-J. Yoon, H.-W. Lee, H.-C. Kim, B.-Y. Lee, O. Hermansen, T.-W. Kim, and K. Holmén (2013), Linking atmospheric dimethyl sulfide and the Arctic Ocean spring bloom, *Geophys. Res. Lett.*, *40*, 155–160, doi:10.1029/2012GL054560.

1. Introduction

[2] Dimethyl sulfide (DMS) is of marine origin, is mostly produced by marine phytoplankton, and is the most abundant

form of sulfur released from the ocean [Stefels *et al.*, 2007]. The oceanic DMS flux, estimated using surface ocean DMS concentration data in conjunction with corresponding air-sea exchange coefficients for DMS, has been reported to be in the range 18–34 Tg yr⁻¹ [Lana *et al.*, 2011], and accounts for 10–40% of the total sulfur flux [Simó, 2001]. Moreover, the annual DMS flux from the Arctic Ocean is predicted to increase by up to 80% by 2080 [Gabric *et al.*, 2005], possibly as a consequence of changes in phytoplankton productivity associated with shoaling of the mixed layer resulting from sea ice melting. However, cause and effect associations among oceanic DMS flux, changes in sea ice extent, and phytoplankton productivity are yet to be established because concurrent measurements of those parameters are not available.

[3] Continuous records of the mixing ratios of atmospheric DMS and its oxidation products near polar regions are only available in Antarctica [e.g., Preunkert *et al.*, 2007]. We are not aware of any comparable measurements in the Arctic region, except for three independent shipboard measurements made in the marine boundary layer, which indicated that atmospheric DMS mixing ratios were closely associated with whether or not given air masses passed over DMS source regions within the marine boundary layer [Lundén *et al.*, 2007]. A similar analysis was performed on limited shipboard atmospheric DMS data collected from the South Atlantic over a short period (<10 days), which established only a partial link between DMS mixing ratios and satellite-derived chlorophyll-*a* (chl-*a*) concentrations [Arnold *et al.*, 2010]. Furthermore, the previous studies have been unable to evaluate how changes in both ocean DMS source strength and multiple meteorological parameters collectively influence the atmospheric DMS mixing ratio on varying time scales (daily to weekly) over the extended period from bloom initiation to termination.

[4] The objectives of the present study were to report accurate measurements of atmospheric DMS mixing ratios determined continuously from April 2010 to March 2011 at Svalbard, Norway (78.5°N, 11.8°E), and to identify the key environmental factors that governed variability in the ratios observed during the entire period of the 2010 spring bloom. This was achieved by analysis of meteorological parameters (air mass back-trajectory, altitude, and speed) and satellite-derived ocean chl-*a* data for regions in the vicinity of Svalbard at the time of the atmospheric DMS measurements.

2. Study Site and Data Sources

2.1. Atmospheric DMS Sampling Site and Ocean Regions in the Vicinity of Svalbard

[5] The atmospheric DMS analytical system was installed in March 2010 at an elevation of 474 m above sea level on

¹School of Environmental Science and Engineering, Pohang University of Science and Technology, Pohang, Korea.

²Korea Polar Research Institute, Incheon, Korea.

³Norwegian Institute of Air Research, Instituttveien 18, Kjeller, Norway.

⁴Norwegian Polar Institute, Fram Centre, Tromsø, Norway.

Corresponding author: K. Lee, School of Environmental Science and Engineering, Pohang University of Science and Technology, Pohang 790-784, Korea. (ktl@postech.ac.kr)

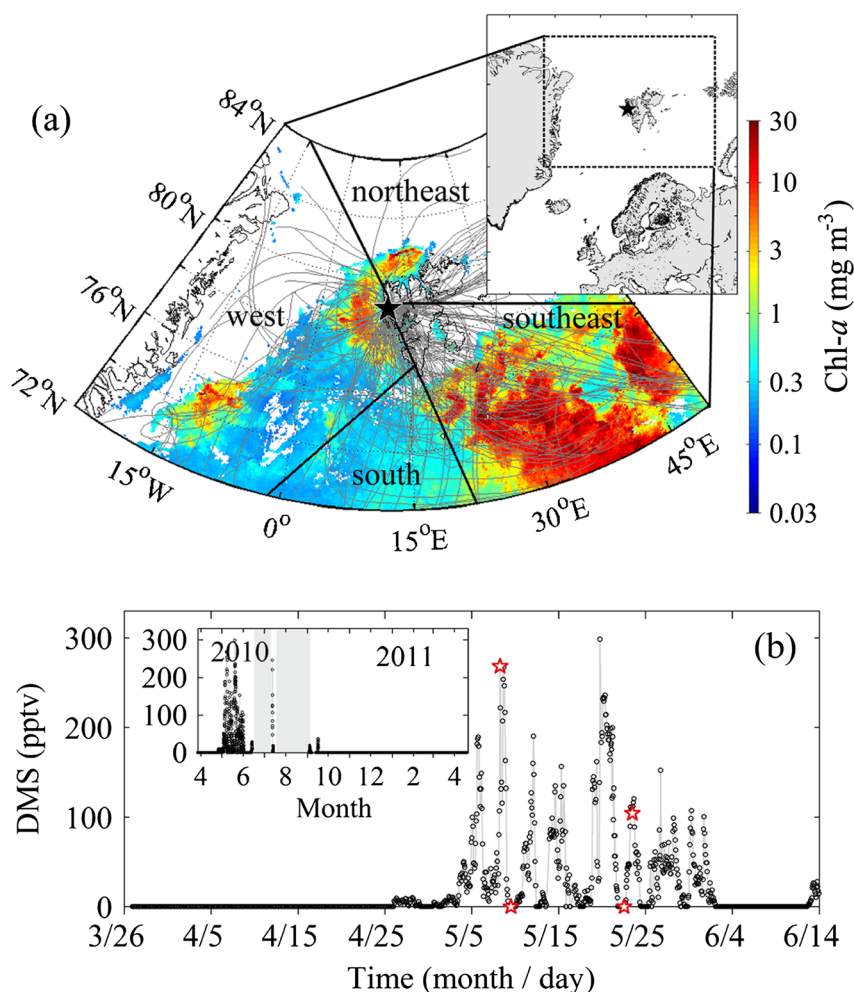


Figure 1. (a) Monthly mean chl-*a* concentration for May 2010 in the study area (between 72°N–84°N and 25°W–50°E) overlaid with the 2 day air mass back-trajectories at 4 h intervals. The solid lines indicate the boundaries of the four subdomains: northeast (low biomass, 0.9 mg m⁻³), southeast (high biomass, 6.7 mg m⁻³), south (low biomass, 0.5 mg m⁻³), and west (high biomass, 2.7 mg m⁻³). The filled star indicates the location of the Zeppelin site (474 m above sea level), Svalbard (78.5°N, 11.8°E). (b) Mixing ratios of atmospheric DMS measured at approximately hourly intervals from 26 March to 13 June 2010 at Zeppelin Station, Svalbard. The atmospheric DMS mixing ratios marked by the open stars correspond to the 2 day air mass back-trajectories shown in Figure 3. The inset shows the DMS mixing ratios measured over a 1 year period (April 2010 to March 2011). The two vertical gray shaded areas in the inset indicate intervals where no measurements were obtained.

Zeppelin Mountain, Svalbard (Figure 1a). Because Svalbard is located 1000 km from the Scandinavian Peninsula, the measurements made at this site were considered to have minimal influence from pollution sources from the European continent, and thus are representative of the remote Arctic Ocean [Lund Myhre et al., 2012].

[6] Based on an accepted rate of DMS oxidation in the Arctic atmosphere (1.8 d^{-1}) [Lundén et al., 2007] and the mean air mass speed for May ($5.8 \pm 2.9 \text{ m s}^{-1}$) we defined the oceanic domain (72°N–84°N and 25°W–50°E; $1.7 \times 10^6 \text{ km}^2$) within which produced DMS was likely to reach the Zeppelin site (Figure 1a). Based on the mean chl-*a* based phytoplankton biomass for May, we further divided it into four smaller subdomains, including the northeast (low biomass, 0.9 mg m⁻³), southeast (high biomass, 6.7 mg m⁻³, located 500 km southeast of the Zeppelin site), south (low biomass, 0.5 mg m⁻³), and west (high biomass, 2.7 mg m⁻³, located immediately west of the Zeppelin site).

The onset of the spring bloom in the study area is known to be strongly associated with break up of the sea ice, increased solar radiation, and thereby increased water column stratification. As a result, most of the annual primary production in this area occurs in spring [Sakshaug, 2004].

2.2. Data Sources (Chl-*a* and Meteorological Data)

[7] The data sets of 8 day mean chl-*a* concentration at a 4 km resolution (acquired from the Level-3 product of the Moderate Resolution Imaging Spectroradiometer (MODIS) on the satellite Aqua) were used to investigate the evolution of phytoplankton biomass in ocean regions near Svalbard from 30 March to 25 June 2010 (see Figure S1 in the Supporting Information). We also used the monthly mean chl-*a* concentration observed from March to September to identify the most productive month during 2010.

[8] Air mass back-trajectories (Figures 1a, 3, and S1) and marine boundary layers (Figures 3 and 4) were calculated

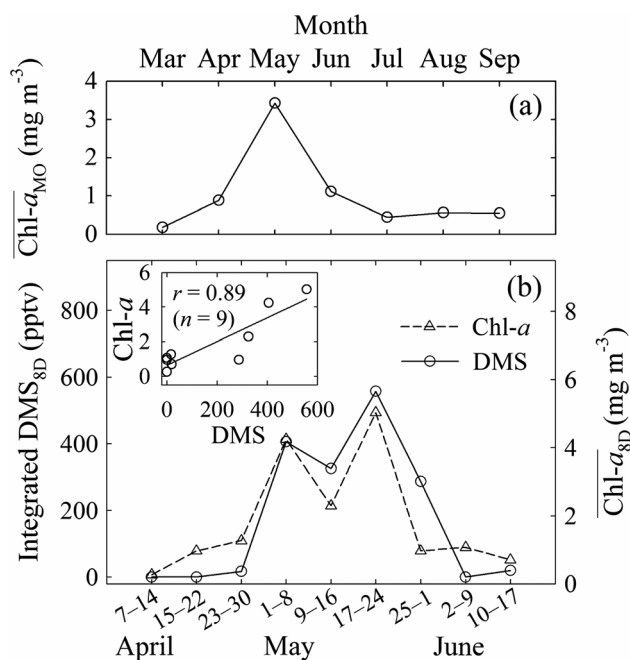


Figure 2. (a) Monthly mean chl-*a* concentrations ($\overline{\text{Chl-}a_{\text{MO}}}$) from March to September 2010. (b) The 8 day mean chl-*a* concentrations ($\overline{\text{Chl-}a_{8\text{D}}}$ open triangles) representing the defined ocean domain (72°N – 84°N and 25°W – 50°E), and the corresponding atmospheric DMS mixing ratios (open circles) measured at Zeppelin Station from early April to mid-June 2010, and integrated over the same period. The inset in Figure 2b showed the correlation between the atmospheric DMS mixing ratios integrated over 8 days and the corresponding mean chl-*a* values from early April to mid-June. The solid line in the inset indicates the best fit.

using the Hybrid Single-Particle Lagrangian Integrated Trajectories model [Draxler and Hess, 1998]. The air mass trajectory data includes the locations of certain air masses over the previous 2 days, recorded at 1–4 h intervals prior to their arrival at Zeppelin Station. The speed of a given air mass was calculated by dividing the distance (km) of the given air mass back-trajectory by the time (hours) taken to produce the air mass back-trajectory. We limited our analysis of air mass trajectories to 2 days prior to the arrival of air masses at the study site, because the mean lifetime of DMS in the Arctic atmosphere has been estimated to be 1.8 days [Lundén et al., 2007].

3. Results and Discussion

[9] The observed atmospheric DMS mixing ratios differed strikingly among seasons (inset in Figure 1b). The DMS mixing ratios determined during the growing season (May to September) increased by 200–300 parts per trillion by volume (pptv) in May, with considerable short-term (< a few days) variability, whereas they remained similar to or less than the analytical detection limit (1.5 pptv DMS) throughout winter (October to April; inset in Figure 1b). We were unable to acquire DMS data from late June to late August because of a malfunctioning in the air intake system. Long-term (one week or longer) and short-term (hours and

days) variability was evident in the DMS mixing ratios found between late April and mid-June (Figure 1b). For this period we evaluate the individual effects of factors influencing this variability at the study site, including changes in the source strength of oceanic DMS; and the trajectory, altitude and speed of air masses arriving at the site.

3.1. The Source Strength of Oceanic DMS

[10] In the ocean domain defined in this study (72°N – 84°N and 25°W – 50°E), the monthly mean chl-*a* concentration for May 2010 was 3.4 mg m^{-3} , which was approximately threefold higher than the values recorded for each of April and June 2010 (Figure 2a). Therefore, our analysis primarily focused on the period from early April to mid-June, which was the period of the greatest phytoplankton biomass. The 8 day mean chl-*a* concentrations in the defined domain progressively increased from early April to early May, reached the highest levels between 1 May and 24 May, and rapidly decreased thereafter (Figure 2b). Temporal variability in the chl-*a* concentration was pronounced in areas immediately west of Svalbard and approximately 500 km distant toward the southwest, where the highest levels of chl-*a* were found (Figure S1).

[11] To evaluate whether the temporal changes in chl-*a* concentration corresponded to variations in the atmospheric DMS mixing ratio measured at Zeppelin Station, we determined the significance of the statistical correlation between the 8 day mean chl-*a* concentrations, representing the defined ocean domain, and the corresponding DMS mixing ratios integrated over the same period. We found that they were highly correlated ($r=0.89$, $P<0.05$) (inset in Figure 2b). The significance of the observed correlation was unanticipated, and indicated that in all of the 8 day intervals shown in Figure 2b, the interval-to-interval variations in other factors (air mass trajectory and altitude) that concurrently influenced DMS mixing ratios were probably insignificant, and therefore could not be driving the variations in the 8 day cumulative atmospheric DMS mixing ratio. This hypothesis is further supported by the observation that during each of the 8 day intervals, the percent number of air masses (2 day back-trajectory at 1 h intervals) that swept through the two productive regions (southeast and west subdomain) was similar ($63 \pm 6\%$). Another notable feature in our analysis is the absence of lag periods between the evolution of DMS mixing ratio and that of chl-*a* concentration. It was reported that DMS is often produced following local chl-*a* maxima, leading to lag periods (on the order of weeks) [Simó, 2001]. This phenomenon is particularly evident when DMS is produced via grazing by zooplankton on DMSP-containing phytoplankton [Stefels et al., 2007]. The absence of lag periods in our study area indicated that variations in chl-*a* concentration are a direct indicator of change in DMS producing phytoplankton biomass.

[12] In ocean waters in the vicinity of Svalbard the major phytoplankton species in spring blooms have been reported to be the prymnesiophyte *Phaeocystis pouchetii* and diatoms, the former in particular produces large amounts of DMS [Degerlund and Eilertsen, 2010; Schoemann et al., 2005]. Therefore, the significance of the correlation (with no lag) between variations in the atmospheric DMS mixing ratio and the chl-*a* concentration indicated that the change in phytoplankton biomass in the defined domain was closely associated with the change in DMS producing phytoplankton

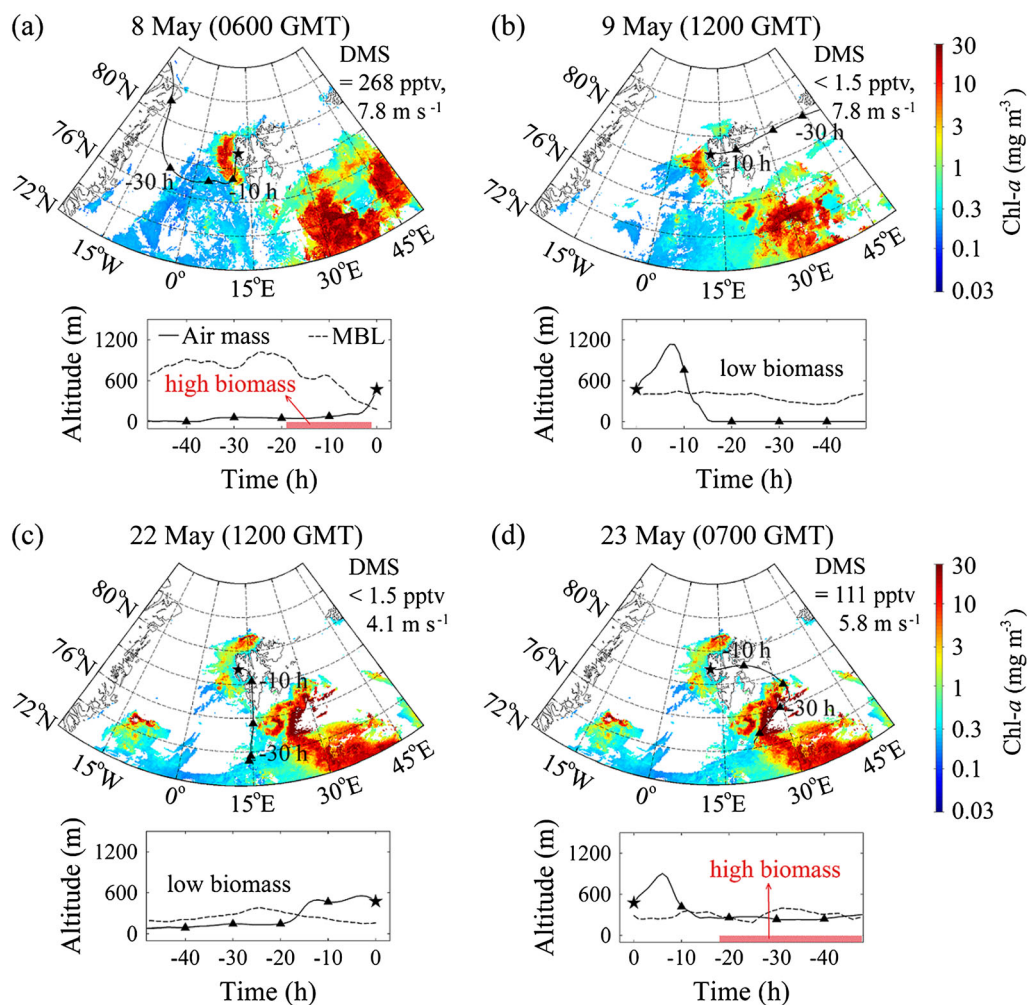


Figure 3. (a–d) Results for 2 day air mass back-trajectories corresponding to the four red stars shown in Figure 1. The four filled triangles marked along the 2 day back-trajectories correspond to 10, 20, 30, and 40 h prior to arrival at Zeppelin Station. The rectangular panels below the figures show the evolution of air mass altitudes and marine boundary layers (MBL) during the 2 day air mass back-trajectories. The atmospheric DMS mixing ratios measured when the air masses arrived at the Zeppelin site are shown in Figures 3a–3d. The 2 day mean air mass speeds are also indicated. Filled stars in the rectangular panels indicate the Zeppelin site.

(probably *P. pouchetii*), and thus was probably a primary influence on long-term (> one week) variations in the DMS mixing ratio measured at Zeppelin Station.

3.2. Meteorological Condition: Air Mass Trajectory and Altitude

[13] The change in the DMS source strength in the chosen ocean domain satisfactorily explained the observed long-term variability in the atmospheric DMS mixing ratios measured at the Zeppelin site. However, it may not be adequate to explain the short-term (hours and days) variability, and thus other factors associated with meteorological condition (air mass trajectory and altitude) were probably concurrently involved because they also vary on time scales of hours and days. To highlight the importance of the involvement of air mass trajectory and altitude in governing the short-term variability, we compared the two sets of air mass back-trajectories estimated over the previous 2 days prior to their arrivals at Zeppelin with the corresponding DMS mixing ratios. The air mass back-trajectories (estimated for 8 May and 23 May) that corresponded to high mixing ratios of DMS coincided

with the regions of high productivity centered immediately to the west of Svalbard and 500 km southeast of Svalbard (Figures 3a and 3d), but the other back-trajectories (estimated for 9 May and 22 May) that corresponded to DMS mixing ratios below the detection limit (1.5 pptv) coincided with regions of low productivity (Figures 3b and 3c). This suggests that for the back-trajectories corresponding to high DMS mixing ratios, the air masses swept through the marine boundary layer over the DMS source regions, transported the DMS released from the ocean sources, and carried it to the Zeppelin site. For the back-trajectories corresponding to DMS mixing ratios that are lower than the detection limit, the air masses were transported over the ocean regions producing little DMS.

[14] An additional analysis was performed to assess the effect of air mass altitude on the atmospheric DMS mixing ratios measured at the Zeppelin site. We chose a window of time during which variations in other factors (DMS source strength and air mass speed) were minimal in each subdomain. We chose the period 1–24 May and 1–16 May as an optimal time window, during which the 8 day mean

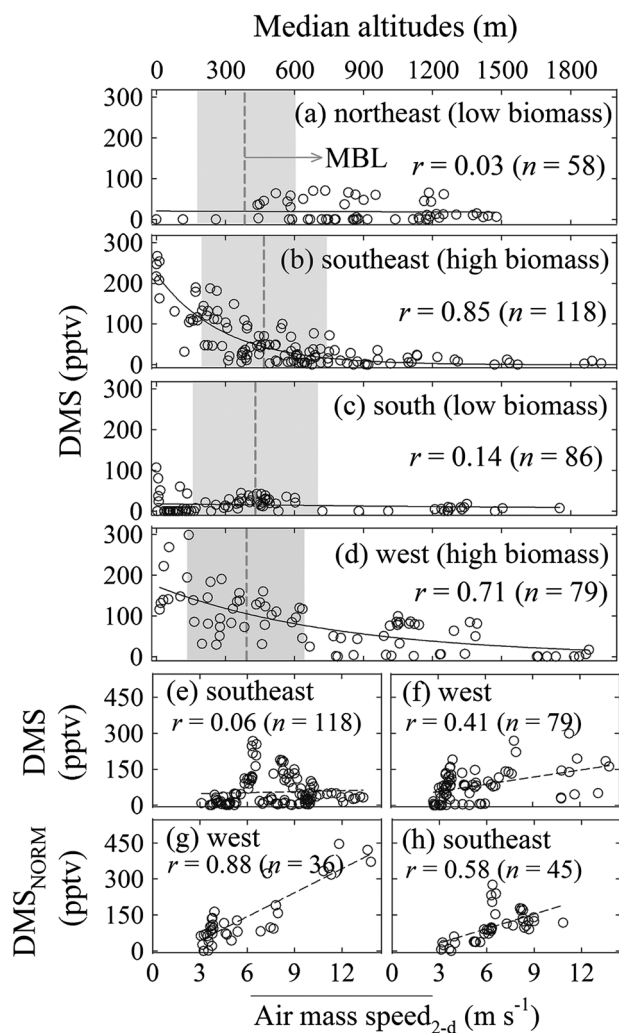


Figure 4. (a–d) Mixing ratios of DMS measured at the Zeppelin site as a function of the median altitude of the air masses associated with each of the four subdomains in the study area. The grey dashed lines and shading indicate the mean marine boundary layers (MBL) and the standard deviations (1σ) from those means, respectively, for each of the subdomains during the analysis period (1–24 May, 1–16 May for the west subdomain). The solid lines represent the best fits. (e, f) Mixing ratio of DMS originating from the productive southeast and west subdomains as a function of the 2 day mean air mass speeds. (g, h) Mixing ratio of chl-*a* normalized DMS (DMS_{NORM}) as a function of the 2 day mean air mass speeds. Air mass trajectories within the marine boundary layer were used to minimize effect of air mass altitude. The dashed lines indicate the best fits.

chl-*a* concentrations representing the productive subdomains of the southeast ($72^{\circ}N$ – $77^{\circ}N$ and $24^{\circ}E$ – $50^{\circ}E$) and west ($76^{\circ}N$ – $80^{\circ}N$ and $4^{\circ}E$ – $10^{\circ}E$), respectively, did not vary more than 30% from the means ($8.9 \pm 2.5 \text{ mg m}^{-3}$ for the southwest, and $4.0 \pm 0.6 \text{ mg m}^{-3}$ for the west). Note that in the same analysis we chose the period 1–24 May for the nonproductive subdomains (northeast and south).

[15] The 2 day air mass back-trajectories estimated at 1 h intervals showed that atmospheric DMS mixing ratios were sensitive to whether or not a given air mass passed over a DMS source region, and the altitude at which the air mass

passed over the source region (Figure 4). The air masses originating from the nonproductive subdomains (northeast and south) predominantly corresponded to <50 pptv DMS (Figures 4a and 4c), and for these air masses no correlation was found between their altitude and the corresponding DMS mixing ratios because DMS production in these subdomains was low during the study period (indicated by chl-*a* $< 1 \text{ mg m}^{-3}$). In contrast, the altitudes of the air masses originating from the productive subdomains (southeast and west) were inversely correlated with the atmospheric DMS mixing ratios measured at the Zeppelin site (Figures 4b and 4d). This is probably because the lower the altitude of an air mass as it passes over an ocean DMS source, the more DMS enters the air mass, thereby increasing the DMS mixing ratios. The correlation between air mass altitudes above DMS source regions and the corresponding DMS mixing ratios measured at the Zeppelin site was highly significant for the southeast ($r=0.85$, $P < 0.05$; Figure 4b) and the west ($r=0.71$, $P < 0.05$; Figure 4d) subdomains.

[16] It is important to note that we were unable to remove or minimize the effect of variations in air mass speed in our analysis (shown in Figures 4b and 4d) because of considerable short-term variations in air mass speed. When the same data sets of atmospheric DMS mixing ratios presented in Figures 4b and 4d were replotted as a function of air mass speed, we found they were not correlated for the southeast ($r=0.06$; Figure 4e), and were less significantly correlated for the west ($r=0.41$; Figure 4f). This result indirectly strengthens our conclusion that the variations in atmospheric DMS mixing ratio shown in Figures 4b and 4d were more closely associated with variations in air mass altitude above DMS source regions than with air mass speed.

3.3. Meteorological Condition: Gas Exchange Rate (Typically Expressed as a Function of Air Mass Speed)

[17] The effect of another meteorological condition (gas exchange rate) on variations in the atmospheric DMS mixing ratio measured at the Zeppelin site may be partially evident in our results (sections 3.1 and 3.2). However, based on the rationale presented in section 3.2, changes in the DMS mixing ratio resulting from variations in air mass speed could only be estimated when all other factors influencing DMS mixing ratios remained approximately unchanged during the analysis period, or when the effect of air mass speed variations overwhelmed the combined effects of variations associated with all other factors. We used the same period (1–24 May) and productive subdomains (southeast and west) that were used in the analysis of air mass altitude (section 3.2); the main differences were the use of air mass trajectories within the marine boundary layer, and the use of chl-*a* normalized DMS mixing ratios ($DMS_{NORM} = DMS \times Chl-a_{24D} / Chl-a_{8D}$, where DMS_{NORM} is normalized DMS, and $Chl-a_{24D}$ and $Chl-a_{8D}$ are the 24 day and 8 day mean chl-*a* concentrations, respectively). This normalization method minimized the effect of differences in the DMS source strength in each subdomain. Thus, we assumed that within this time window the effect of air mass speed variations on mixing ratios of DMS measured at the Zeppelin site was far greater than that of other factors (i.e., DMS source strength, and air mass trajectory and altitude). The ocean DMS source immediately to the west of Svalbard largely met the criteria for our analysis because most of air masses

passing over this source region were at similar altitudes (approximately within the marine boundary layer), but had varying speeds (3–13 m s⁻¹) prior to reaching the Zeppelin site. In addition, the possible loss of DMS because of photochemical oxidation was probably minimal, or similar in magnitude within the selected time window because of the proximity of this DMS source to the Zeppelin site.

[18] In this analysis we found a strong positive relationship between the atmospheric DMS mixing ratios and air mass speed for air masses originating from the west subdomain in the range 3–13 m s⁻¹ ($r=0.88$, Figure 4g). We also found a comparable correlation between DMS mixing ratios and air mass speed for air masses originating from the southeast subdomain ($r=0.58$, Figure 4h). This was not anticipated, because factors other than air mass speed (air mass altitude, photo-oxidation of DMS, mixing with other air masses with different DMS mixing ratios) were likely to be involved in influencing DMS mixing ratios during the 500 km passage of the air masses from the southeast domain to the Zeppelin site. If the influences of all other factors were comparable to or greater than the effect of air mass speed, they would have made the correlation ambiguous. Although the data in Figures 4g and 4h were reasonably correlated with air mass speed, the relationship between these variables is likely to be nonlinear because the amount of DMS flux from the ocean is nonlinearly related with air mass speed; however, the data are insufficient to extract the exact relation (linear or polynomial).

[19] We were not able to investigate the effects of removal of DMS through oxidation mechanism [Ayers and Gillett, 2000] due to lack of measurements of oxidizing species or DMS oxidation products. However, given the strong relationships observed with air mass altitude, trajectory, and speed any signal in DMS concentration would likely be overwhelmed.

4. Conclusion

[20] The atmospheric DMS mixing ratios measured at the Zeppelin site (Svalbard, Norway) reasonably represented the evolution of the phytoplankton community and meteorological conditions (air mass trajectory, altitude, and speed) in relation to in situ production and release of DMS in the Arctic Ocean surrounding the study site. We found a strong and positive correlation between atmospheric DMS mixing ratios and chl-*a* concentrations between early April and mid-June, suggesting that temporal variations in chl-*a* concentration (a measure of total phytoplankton biomass) in waters in the vicinity of Svalbard reflected variations in the abundance of DMS producers. Our analysis also indicates that variations in the DMS mixing ratio occurring on time scales longer than one week were largely associated with temporal changes in the strength of the ocean DMS source, while variations occurring on shorter time scales were more closely associated with the trajectory, altitude, and speed of air masses reaching the Zeppelin site. One important implication of our results is that in similar future studies satellite-

derived chl-*a* concentrations can be used as an indicator of the abundance of DMS-producing phytoplankton in polar oceans where blooms of DMS producers (e.g., *Phaeocystis*) are frequent and widespread [Smith *et al.*, 1991].

[21] **Acknowledgment.** We would like to thank Martin Johnson, an anonymous reviewer and Associate Editor Pete Strutton for providing insightful comments, which greatly helped us to increase the readability of the manuscript. The preparation of the manuscript was supported by the Mid-career Research Program of the Korea National Research Foundation (2012R1A2A1A01004631) and by Polar Academy Program of the Korea Polar Research Institute. Partial support was also provided by the project titled “Long-term change of structure and function in marine ecosystems of Korea” funded by the Ministry of Land, Transport and Maritime Affairs and by Korea Polar Research Institute (PE12290). We thank the Sverdrup Research Station staffs of the Norwegian Polar Institute for assisting us to set up the atmospheric DMS analysis system at Zeppelin station.

References

- Arnold, S. R., D. V. Spracklen, S. Gebhardt, T. Custer, J. Williams, I. Peeken, and S. Alvaín (2010), Relationships between atmospheric organic compounds and air-mass exposure to marine biology, *Environ. Chem.*, 7(3), 232–241, doi:10.1071/EN09144.
- Ayers, G. P., and R. W. Gillett (2000), DMS and its oxidation products in the remote marine atmosphere: Implications for climate and atmospheric chemistry, *J. Sea Res.*, 43, 275–286.
- Draxler, R. R., and G. D. Hess (1998), An overview of the HYSPLIT 4 modelling system for trajectories, dispersion and deposition, *Aust. Meteorol. Mag.*, 47(4), 295–308.
- Degerlund, M., and H. C. Eilertsen (2010), Main species characteristics of phytoplankton spring blooms in NE Atlantic and Arctic waters (68–80°N), *Est. Coasts.*, 33, 242–269.
- Gabric, A. J., B. Qu, P. Matrai, and A. C. Hirst (2005), The simulated response of dimethylsulfide production in the Arctic Ocean to global warming, *Tellus, Ser. B*, 57(5), 391–403.
- Lana, A., et al. (2011), An updated climatology of surface dimethylsulfide concentrations and emission fluxes in the global ocean, *Global Biogeochem. Cycles*, 25, GB1004, doi:10.1029/2010GB003850.
- Lundén, J., G. Svensson, and C. Leck (2007), Influence of meteorological processes on the spatial and temporal variability of atmospheric dimethyl sulfide in the high Arctic summer, *J. Geophys. Res.*, 112, D13308, doi:10.1029/2006JD008183.
- Lund Myhre, C., et al. (2012), Monitoring of greenhouse gases and aerosols at Svalbard and Birkenes: Annual report 2010, Norwegian Institute for Air Research, TA-2902/2012.
- Preunkert, S., M. Legrand, B. Jourdain, C. Moulin, S. Belviso, N. Kasamatsu, M. Fukuchi, and T. Hirawake (2007), Interannual variability of dimethylsulfide in air and seawater and its atmospheric oxidation by-products (methanesulfonate and sulfate) at Dumont d’Urville, coastal Antarctica (1999–2003), *J. Geophys. Res.*, 112, D06306, doi:10.1029/2006JD007585.
- Sakshaug, E. (2004), Primary and secondary production in the Arctic Seas, in *The Organic Carbon Cycle in the Arctic Ocean*, edited by Stein R, and R. W. Macdonald, pp. 57–81, Springer, Berlin.
- Schoemann, V., S. Becquevort, J. Stefels, V. Rousseau, and C. Lancelot (2005), *Phaeocystis* blooms in the global ocean and their controlling mechanisms: A review, *J. Sea Res.*, 53, 43–66, doi:10.1016/j.seares.2004.01.008.
- Simó, R. (2001), Production of atmospheric sulfur by oceanic plankton: Biogeochemical, ecological and evolutionary links, *Trends Ecol. Evol.*, 16(6), 287–294, doi:10.1016/S0169-5347(01)02152-8.
- Smith, W. O., Jr., L. A. Codispoti, D. M. Nelson, T. Manley, E. J. Buskey, H. J. Niebauer, and G. F. Cota (1991), Importance of *Phaeocystis* blooms in the high-latitude ocean carbon cycle, *Nature*, 352, 514–516, doi:10.1038/352514a0.
- Stefels, J., M. Steinke, S. Turner, G. Malin, and S. Belviso (2007), Environmental constraints on the production and removal of the climatically active gas dimethylsulphide (DMS) and implications for ecosystem modeling, *Biogeochemistry*, 83, 245–275.